Fusion of proinsulin-producing bone marrow-derived cells with hepatocytes in diabetes

Mineko Fujimiya*†, Hideto Kojima†‡, Masumi Ichinose*, Ryohachi Arai*, Hiroshi Kimura‡, Atsunori Kashiwagi§, and Lawrence Chan†¶

Departments of *Anatomy, ‡Molecular Genetics in Medicine, and §Medicine, Section of Endocrinology and Metabolism, Shiga University of Medical Science, Otsu, Shiga 520-2192, Japan; and †Division of Diabetes, Endocrinology, and Metabolism, Departments of Medicine and Molecular and Cellular Biology, Baylor College of Medicine, One Baylor Plaza, Houston, TX 77030

Communicated by Salih J. Wakil, Baylor College of Medicine, Houston, TX, January 9, 2007 (received for review November 6, 2006)

We previously reported that diabetes in mice is associated with the appearance of proinsulin-producing (Proins-P) cells in the liver. It was unclear, however, whether these Proins-P bone marrow-derived cells (BMDC) merely transit through the liver or undergo fusion with hepatocytes, normally an extremely rare event. In this study, we found that, in diabetes, BMDC in the liver produce not only Proins but also TNF-α, suggesting that diabetes reprograms gene expression in BMDC, turning on ''inappropriate'' genes. Bone marrow transplantation using genetically marked donor and recipient mice showed that fusion occurs between Proins-P BMDC and hepatocytes. Cell fusion is further supported by the presence of the Y chromosome in Proins-P cells in female mice that received male bone marrow transplantation cells. Morphologically, Proins-P fusion cells are albumin-producing hepatocytes that constitute $\approx$2.5% of the liver section area 5 months after diabetes induction. An extensive search failed to reveal any fusion cells in nondiabetic mice. Thus, diabetes causes fusion between Proins-P BMDC and hepatocytes *in vivo*, an observation that has implications for the pathophysiology of diabetes as well as the fundamental biology of heterotypic cell fusion.

cell fusion | diabetes mellitus | diabetic complications | liver

Recent reports from different laboratories document that bone marrow-derived cells (BMDC) can fuse with hepatocytes *in vivo*, and such fusion events can contribute to liver regeneration (1–4). However, with the exception of unique genetic models, e.g., fumarylacetoacetate hydrolase (Fah)-deficient mice (1, 2), in which wild-type BMDC confer a marked growth advantage, BMDC–hepatocyte fusion appears to be extremely rare. In a review article, Thorgeirsson and Grisham (5) estimated that transplanted BMDC generate hepatocyte-like cells in the liver at a frequency of $\leq 10^{-4}$. In fact, the yield of presumed BMDC–hepatocyte fusion cells ranges from 0 to $<$0.05% in $>$80% of reports published before August 2005 (5). Apart from the rarity of the event, there is little information on whether BMDC–hepatocyte cell fusion is regulated by physiological body functions, and whether it is affected by pathological conditions other than the extreme example of Fah-deficient mice that received bone marrow transplantation (BMT) from Fah-expressing mice.

Our laboratory recently reported the appearance of proinsulin-producing (Proins-P) cells in the bone marrow of diabetic rats and mice (6). The Proins-P BMDC migrate out of the bone marrow and populate different organs and tissues, including liver and fat. Because the phenomenon occurs in both type 1 and type 2 models, and can be duplicated by glucose injections in mice, hyperglycemia appears to trigger its occurrence. This interpretation is supported by the observation that $\approx$50% of unfractionated BMDC start transcribing insulin within days of incubation in high-glucose medium (7).

Diabetes mellitus is a prevalent disease that affects $\approx$7% of the U.S. population and a rapidly growing proportion of the world population (8). The fact that hyperglycemia *per se* causes the Proins-P BMDC to appear in the liver prompted us to ask whether these cells actually fuse with liver cells and, if they do, at what frequency. Fusion would also be relevant to the residence time (explaining the presence) of BMDC in the liver but not in many other organs (6). We found that, indeed, fusion occurs between BMDC and hepatocytes in diabetic mice with a frequency that is at least $>$100- to 1,000-fold higher than that in nondiabetic controls. Thus, diabetes, a common pathological condition, produces major perturbations in the behavior of BMDC that may have significant pathophysiological implications.

Results

Proinsulin-Producing Cells in the Liver of Streptozotocin (STZ)-Diabetic Mice. We produced diabetes in 8-week-old C57BL/6 mice by i.p. STZ injection and studied the diabetic mice 2 months later. By immunostaining, we found the presence of Proins-P cells in the liver of these mice but not of sham-treated nondiabetic controls [see ref. 6 and supporting information (SI) Fig. 6]. *In situ* nucleic acid hybridization revealed the presence of proinsulin transcripts in STZ-diabetic and not control mouse liver (SI Fig. 6 *c–f*), indicating that cells in the liver of diabetic animals have the potential to synthesize proinsulin, and the immunostaining comes from proinsulin production *in situ* and not its uptake from the circulation. At 2 months after STZ, 1.1 $\pm$ 0.4% of the liver sections were occupied by Proins-P cells. At 5 months, the total area of Proins-P cells increased to 2.5 $\pm$ 1.1%, and at 8 months, it stayed at 2.5 $\pm$ 0.1%. As noted previously, the Proins-P cells do not secrete sufficient insulin to affect directly the glucose homeostasis of the diabetic mice. However, they are a convenient marker for a subpopulation of BMDC formed in response to the hyperglycemia (see below and ref. 6).

Bone Marrow Origin of Proins-P Cells in the Livers of Diabetic Mice. We next performed BMT from GFP mice (transgenic mice that constitutively express GFP) to Rosa mice (transgenic mice that constitutively express β-gal), induced diabetes in the BMT recipients with STZ and examined their livers 8 weeks later. Immunohistochemical analysis revealed the presence of GFP-positive BMDC scattered in liver sections of both diabetic and nondiabetic mice (Fig. 1 *a–c* and *g–i*). On higher-magnification (Fig. 1 *d–f* and *j–l*), only in diabetic mice did we find evidence of overlap staining of GFP with β-gal immunoreactivity (which

Author contributions: M.F. and H. Kojima contributed equally to this work; M.F., H. Kojima, and L.C. designed research; M.F., H. Kojima, and M.I. performed research; R.A., H. Kimura, and A.K. contributed new reagents/analytic tools; M.F., H. Kojima, and L.C. analyzed data; and M.F., H. Kojima, and L.C. wrote the paper.

The authors declare no conflict of interest.

Abbreviations: BMDC, bone marrow-derived cells; BMT, bone marrow transplantation; Proins-P, proinsulin-producing; STZ, streptozotocin.

¶To whom correspondence should be addressed. E-mail: lchan@bcm.edu.

This article contains supporting information online at www.pnas.org/cgi/content/full/0700220104/DC1.

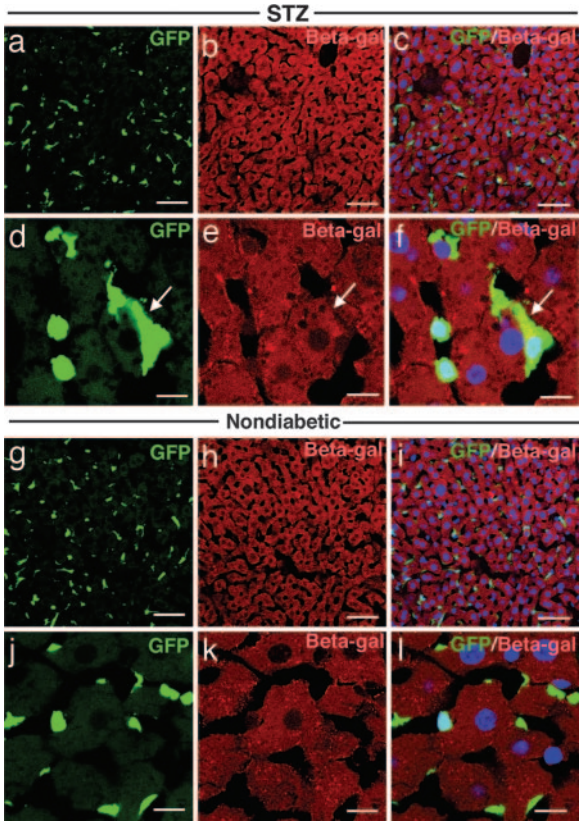

Fig. 1. Overlap images of GFP and β-gal-positive reactions in liver sections of STZ-diabetic (*a–f*) and nondiabetic (*g–l*) ROSA mice that had received BMT from GFP-mice. GFP-expressing cells are widely scattered in the liver in both diabetic (*a* and *d*) and nondiabetic (*g* and *j*) liver sections. At high magnification, in diabetic liver, GFP reaction overlaps that of β-gal staining in the cytoplasm of hepatocytes (*f*) of diabetic mice but not in nondiabetic mice (*l*). [Scale bars: 50 μm (*a–c* and *g–i*) and 10 μm (*d–f* and *j–l*).]

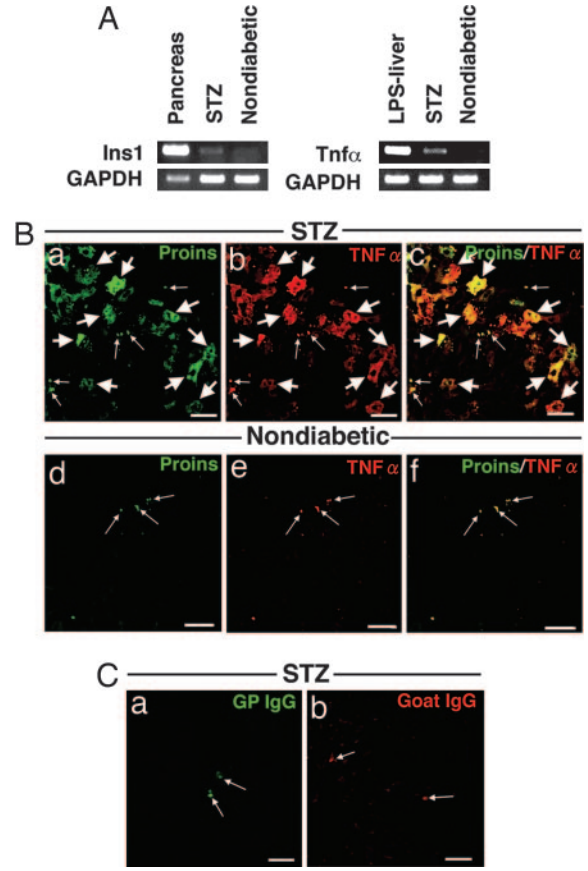

Fig. 2. Expression of proinsulin and TNF-α in the livers of diabetic mice. (*A*) RT-PCR analysis for insulin 1 (Ins 1) and TNF-α in liver from STZ-diabetic or nondiabetic mice. Positive controls are RNA from pancreas (Ins1) or LPS-treated mouse liver. (*B*) Immunofluorescence overlap staining of Proins and TNF-α in the liver of STZ-diabetic (*a–c*) and nondiabetic (*d–f*) wild-type mice. Most Proins-positive cells in the liver also coexpress TNF-α (large arrows in *a–c*) in STZ-diabetic mice. Tiny specks of fluorescence are occasionally detected in both STZ-diabetic and nondiabetic liver (small arrows in *a–f*), most of which appear to be autofluorescence (see SI Fig. 7). (Scale bars: 50 μm.) (*C*) Control study for fluorescence-positive staining. STZ-diabetic liver was stained with FITC-labeled guinea pig IgG or Cy3-labeled goat IgG without first antibody. There is no specific staining except tiny specks of autofluorescence (arrows). (Scale bars: 50 μm.)

marks cells of recipient mice, Fig. 1*f*), suggestive of BMDC–hepatocyte fusion cells in these mice. GFP and β-gal coexpression was not detected after an extensive search in nondiabetic liver sections (Fig. 1 *g–i*), indicating that, in the absence of diabetes, fusion of BMDC and liver cells, if it occurs at all, is a very rare event.

Diabetes-Induced Proins-P BMDC also Express TNF-α. By RT-PCR, we found expression of both proinsulin and TNF-α mRNA in the livers of diabetic mice (Fig. 2*A*). Confocal laser microscopy and immunofluorescence staining revealed that Proins and TNF-α expression largely overlapped in the same cells (Fig. 2*B*). Nondiabetic mice displayed no evidence of insulin or TNF-α mRNA by RT-PCR (Fig. 2A). Immunofluorescence staining revealed only occasional tiny specks of fluorescence that was very different from the major staining pattern observed in diabetic mice (Fig. 2*B*, see below).

To confirm the bone marrow origin of TNF-α-expressing cells, we examined Rosa mice after they had received BMT from GFP donors and STZ-diabetes induction. Confocal laser microscopy demonstrated coexpression of GFP (indicating BMDC origin), Proins, and TNF-α in the livers of diabetic recipients (Fig. 3 *d* and *h*). In contrast, in nondiabetic controls that had undergone BMT, despite the presence of many GFP-positive cells (BMDC from GFP donors) scattered in the liver of recipient animals (Fig. 3 *i* and *m*), these cells never showed overlap staining with β-gal staining (marking recipient liver cells). We also failed to detect any Proins-P cells in the livers of nondiabetic mice.

The demonstration of immunoreactive proinsulin and TNF-α required the use of an antigen-specific first antibody; in its absence, the fluorescent signals in the livers of diabetic mice are almost completely gone (Fig. 2*C*), indicating the specificity of the reaction (see below). However, tiny scattered specks of fluorescence were detectable in occasional sections in the absence of first antibody (Fig. 2*C a* and *b*, small arrows) and also in sections of nondiabetic mouse liver with or without first antibody (Fig. 2*B d–f*, small arrows). We tested the hypothesis that these signals represent nonspecific autofluorescence.

BMT and Spectral Analysis Confirm the Presence of Proins-P Cells in the Livers of Diabetic Mice. Whether a fluorescent signal comes from GFP is betrayed by its spectral emission pattern. We first examined the fluorescence signals of GFP in the pancreases of nondiabetic MIP-GFP mice [that express GFP driven by the mouse insulin promoter (9)]. The green fluorescence in pancreatic β cells displayed a spectral emission profile with a peak at 507–512 nm, as predicted for GFP (SI Fig. 7 *e* and *f*). We next analyzed the green fluorescent signals in the liver of diabetic MIP-GFP mice 8 weeks after STZ. Confocal laser microscopy

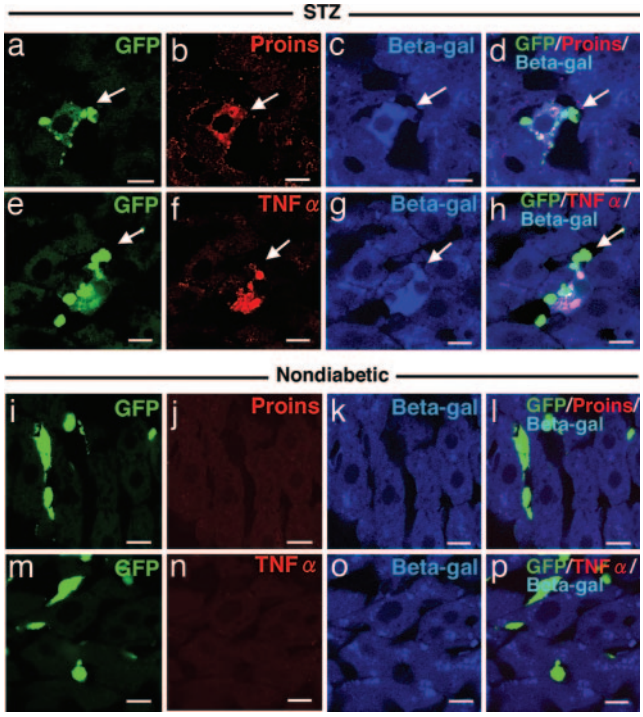

Fig. 3. Overlap image of GFP/Proins/β-gal reaction or GFP/TNF-α/β-gal reaction in liver sections from STZ-diabetic (*a–h*) and nondiabetic (*i–p*) ROSA mice that had received BMT from GFP-mice. GFP/β-gal-coexpressing cells always stained positive for Proins (*d*) and/or TNF-α (*h*) in diabetic liver. In nondiabetic liver, we observed no GFP/β-gal-coexpressing cells (*l* and *p*). Proins- or TNF-α-positive cells were not found in nondiabetic liver (*j* and *n*). (Scale bars, 10 μm.)

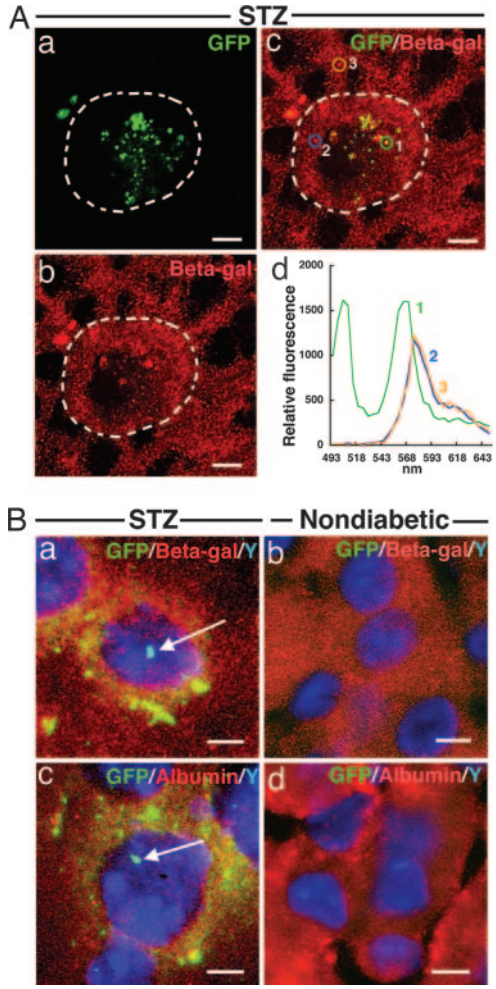

Fig. 4. Fusion of BMDC with hepatocytes. (*A*) Overlap images of GFP and β-gal in the liver of STZ-diabetic ROSA mice that had received BMT from MIP-GFP mice. Punctate pattern of green fluorescence is found in the cytoplasm of hepatocytes (*a*) that also coexpress β-gal (*b* and *c*). Emission spectral profile of green fluorescence is characteristic of that for GFP fluorescence (502–507 nm, d curve-1) and that of β-gal marked by Cy3-labeled antibody (568–573 nm, d curves-2 and 3). Note that curve 1 shows overlap characteristics of both GFP and Cy3 emission spectral profiles. (Scale bars: 10 μm.) (*B*) FISH analysis for Y chromosome and overlap image with β-gal or albumin immunostaining in the liver of female ROSA mice that had received BMT from male MIP-GFP mice. In STZ-diabetic mice, Y chromosome staining is found in the nuclei of the cells that express GFP in the cytoplasm (arrows in *a* and *c*). Double Y chromosome/GFP-positive reactions colocalize with β-gal (*a*) or albumin (*c*) immunostaining in the same cell. Neither Y chromosome nor GFP-positive reaction was found in liver cells of nondiabetic controls (*b* and *d*). (Scale bars: 10 μm.)

revealed an uneven distribution of green fluorescence; the emission spectrum of the strongest fluorescent areas was that of GFP (SI Fig. 7 *a* and *b*). In STZ-diabetic and nondiabetic MIP-GFP mice, as well as in STZ-diabetic and nondiabetic wild-type mice, we observed occasional low level green-yellow fluorescent structures in the liver (SI Fig. 7 *c*, *g*, and *i*); spectral analysis revealed a nonspecific, low level broad spectral profile different from that of GFP (SI Fig. 7 *d*, *h*, and *j*). The area density of such nonspecific fluorescent signals was low compared with the GFP-positive areas, although it was increased in STZ-diabetic mice 2 months after diabetes (0.47 ± 0.06% liver) as compared with that in nondiabetic animals (0.28 ± 0.02% liver). The reason for the small increase in nonspecific fluorescence in diabetes is unknown. Despite extensive search, we failed to detect any fluorescent signal with GFP type of emission spectrum in the liver of nondiabetic mice.

Proins-P BMDC Undergo Fusion with Hepatocytes in Diabetic Mice. Fusion between BMDC and hepatocytes is an extremely rare event in normal mice (5), a conclusion also supported by the lack of overlap staining of GFP donor-BMDC and Rosa recipient liver cells (Fig. 1 *g–l*, see above). Because Proins-P BMDC are present at a substantial density in the livers of diabetic mice (≈1–2.5% in 2- to 8-month-old diabetic mice, see above), we asked whether cell fusion has occurred between Proins-P BMDC and hepatocytes in these animals. Although Fig. *1 a–f* strongly suggests that fusion may have occurred, we sought to corroborate the finding with spectral analysis. We transplanted bone marrow cells from MIP-GFP donor mice (Proins-P cells would be marked by GFP expression) to Rosa recipients. Confocal laser microscopy of liver sections of recipient mice after diabetes induction revealed punctate fluorescent structures in the cytoplasm of hepatocytes that also express β-gal (Fig. 4 *Aa–Ac*). Authenticity of GFP expression was confirmed by its characteristic spectral emission pattern with a peak at 502–507 nm (Fig. 4*Ad*). To identify β-gal-positive cells of recipient mice, we used rabbit anti-β-gal first antibody and Cy3-labeled anti-rabbit IgG second antibody for immunostaining. This strategy allowed us to document β-gal expression by the characteristic Cy3 spectral pattern (with a peak at 568–573 nm, spectra 2 and 3, Fig. 4 *Ac* and *Ad*) with evident overlap with GFP expression.

To obtain additional independent evidence that cell fusion has indeed occurred, we performed BMT between male MIP-GFP donors to female Rosa recipient, and produced diabetes in the recipients by STZ. We detected by FISH the presence of the Y chromosome in the nuclei of the same cells that harbored GFP and β-gal in the cytoplasm (Fig. 4*Ba*, arrow). These cells are

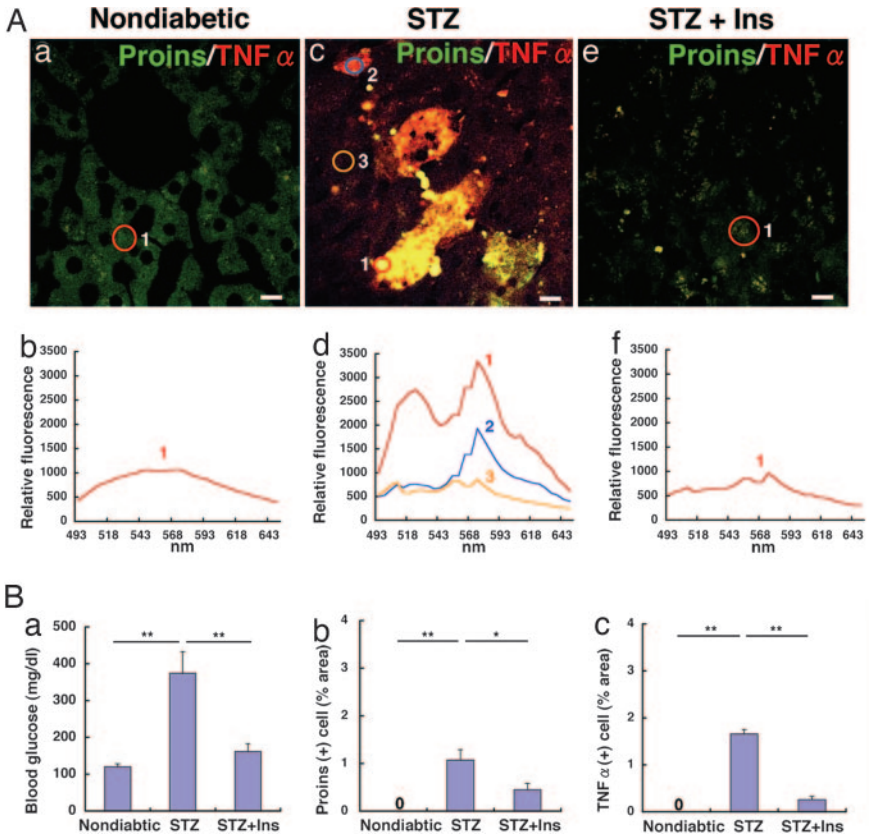

Fig. 5. Insulin treatment inhibits the appearance of proinsulin/TNF-α-positive cells in the livers of diabetic mice. (*A*) Confocal laser microscopy (C1si; Nikon) images of liver sections. Imunofluorescence overlap staining of Proins and TNF-α in the livers of nondiabetic (*a*), STZ-diabetic (*c*) and insulin-treated STZ-diabetic wild-type (*e*) mice. The number of Proinsulin/TNF-α-positive cells seen in the liver of STZ-diabetic mice (*c*) is markedly reduced in insulin-treated STZ-diabetic liver (*e*). (Scale bars: 10 μm.) The emission spectral analysis of Proins/TNF-α-positive area (*c*, circle 1) reveals a double peak specific for both FITC (522 nm) and Cy3 (572 nm), respectively (*d*, curve-1). A few cells are positive for TNF-α only, with a spectral mission profile specific for Cy3 (*c* and *d*, circle and curve-2). (*B*) Blood glucose levels (*a*), percentage area density of Proinsulin-positive cells (*b*) and TNF-α-positive cells (*c*) in the livers of nondiabetic, STZ-diabetic, and insulin-treated STZ-diabetic mice. Values are means ± SEM ($n = 3$). *, $P < 0.05$; **, $P < 0.01$.

hepatocytes by morphology; furthermore, they produce albumin, a hepatocyte-specific protein, in the cytoplasm (albumin labeled red in Fig. 4*Bc*, arrow indicates Y chromosome). In nondiabetic control BMT recipients, neither GFP nor the Y chromosome was found in any of the hepatocytes, which stained positive for β-gal and albumin (Fig. 4 *Bb* and *Bd*).

Proins-PBMDC in MIP-GFP Mice Harbor GFP, Ins1, and TNF-α Transcripts. We performed laser capture microdissection (LCM) to confirm the coexpression of GFP, Ins1, and TNF-α in specific regions of the liver of MIP-GFP mice. We first used confocal laser microscopic analysis, followed by LCM isolation of RNA. RT-PCR analysis of these samples confirmed the coexpression of these molecules observed by microscopy. (*SI Text* and SI Fig. 8).

Insulin Treatment Prevents the Appearance of Proins-P BMDC in the Livers of Diabetic Mice. To ensure that diabetes, and not STZ toxicity, leads to the appearance of Proins-P BMDC in the liver, we treated a group of mice 2 days after STZ treatment with insulin, significantly reducing hyperglycemia (Fig. 5*Ba*). Immunofluorescence-overlap staining coupled with spectral analysis showed that the density of the Proins-P cells and TNF-α-positive BMDC in diabetic mice at 2 months (Fig. 5 *Ac* and *Ad*) was substantially reduced by insulin treatment (Fig. 5 *Ae* and *Bb* and *c*). Thus, the degree of hyperglycemia, and not STZ toxicity, correlates with the induction of Proins and TNF-α gene expression of BMDC in the liver.

Discussion

Postnatal heterotypic liver cell fusion is extremely rare (5), and there is no information on its regulation by common pathophysiological processes. In this study, we tested the hypothesis that a common disorder, diabetes mellitus, may cause BMDC–hepatocyte fusion *in vivo*. We advanced this hypothesis because of the unexpected observation that type 1 and type 2 diabetes in mice and rats leads to the appearance of Proins-P cells outside the pancreas. These cells originate from the bone marrow and populate the liver and fat (6). We designed experiments to determine whether the Proins-P cells in the liver represent BMDC transiting the hepatic circulation or whether they have actually fused with hepatocytes. Moreover, if BMDC do fuse with liver cells, what is the frequency of BMDC–hepatocyte fusion events in diabetes, whether such events occur in the absence of diabetes, and, if they do, at what frequency.

We performed BMT between mice transgenic for different marker genes (summarized in Table 1) and found that, indeed, Proins-P BMDC undergo fusion with hepatocytes in diabetic mice, a conclusion based on combinations of genetic markers that specifically tag the cells of donor and recipient origin; markers used include transgenic proteins, e.g., GFP and β-gal, a natural protein marker, albumin, and the unique diabetes-induced BMDC marker, proinsulin (6), as well as the Y chromosome coming from male BMT donor cells detected in female recipient hepatocytes. In confirmation of the extreme rarity of fusion between BMDC and hepatocytes in normal animals (5),

Table 1. Mouse genotypes and analyses performed

Donor	Recipient	Nondiabetic and STZ-diabetic 2M	5 M and 8 M
No	C57/BL6 wild type	DAB for Proins, *in situ* hybridization, adsorption study, confocal microcopy for Proins/TNF-α and spectral analysis, RT-PCR	Confocal microscopy for Proins or TNF-α
No	MIP-GFP	Spectral analysis for confocal microscopy, LCM and quantitative real-time RT-PCR,	ND
GFP	Rosa	Confocal microscopy for GFP/β-gal, GFP/Proins/β-gal or GFP/Tnf-α/β-gal	ND
Male MIP-GFP	Female Rosa	Confocal microscopy for GFP/β-gal and spectrum analysis, Y chromosome staining combined with GFP/β-gal or GFP/albumin	ND

No donor means no BMT; M, months after STZ-induced diabetes; ND, not done; MIP-GFP, transgenic mice expressing GFP driven by the mouse insulin promoter; Rosa, transgenic mice with constitutive β-gal expression; GFP, transgenic mice with constitutive GFP expression.

the same experimental strategies that documented fusion cells in diabetic mice failed to reveal a single instance of fusion between BMDC and hepatocytes in nondiabetic mice.

In the only other tissue in which diabetes-associated fusion cells occur is the nervous system, in which fusion between BMDC and nerve cells appears to be important in the pathogenesis of diabetic neuropathy (10). Poorly controlled diabetes is associated with liver dysfunction (11, 12) and increased prevalence of significant hepatic pathologies, including cirrhosis (13) and hepatocellular carcinoma (14–16). We surmise that fusion of BMDC with hepatocytes in diabetes renders the latter susceptible to these pathologies, given the fact that cell fusion may contribute to carcinogenesis and other cellular abnormalities (17–19). To date, there is little information on the factors that control heterotypic fusion between BMDC and cells in liver, brain, or heart (1–3, 10, 20–22). Herein, we have uncovered that diabetes, a common pathological condition, is a potent inducer of heterotypic cell fusion *in vivo*. Cell–cell fusion is crucial to normal embryonic development. In adult animals, heterotypic fusion is rare and usually occurs between specialized cells, e.g., sperm–egg (23). Most mature differentiated cells seem to guard against spontaneous heterotypic fusion, which could have detrimental consequences (10, 17–19). Thus, the BMDC–hepatocyte fusion in mice is noteworthy, being observed only in diabetic mice and not in nondiabetic animals. Furthermore, the frequency of $\approx$2.5% is remarkable as compared with the other well documented BMDC–Purkinje cell fusion which has a frequency of $\leq$0.1% (21).

In conclusion, diabetes is associated with fusion between Proins-P BMDC and hepatocytes in mice. Fusion occurs rarely, if at all, in the absence of diabetes. Moreover, in addition to turning on proinsulin expression, the diabetic state also induces TNF-α expression in BMDC, consistent with diabetes causing reprogramming of bone marrow cells to express "inappropriate" genes. We speculate that among these are fusion-promoting genes, and dysregulated gene expression in BMDC and/or hepatocytes predisposes them to fuse with each other (24). Thus, diabetes-induced abnormal gene expression is important not only from the standpoint of the pathophysiology of diabetes (25–27) but also from the standpoint of the fundamental biology of cell fusion and its regulation (24).

Methods

Animals and BMT. Wild-type (C57BL/6JJcl, CLEA Japan, Tokyo, Japan) mice, ROSA (B6.129S7-Gt(ROSA)26Sor/J, The Jackson Laboratory, Bar Harbor, ME) mice, MIP-GFP mice (9) and GFP Tg mice (C57BL/6-Tg(UBC-GFP) 30 Scha, The Jackson Laboratory) were used. Diabetes was induced by i.p. STZ (150 mg/kg) at 8 weeks of age, and diabetic animals were used for experiments at 2, 5, or 8 months later. For BMT, female ROSA mice were irradiated (9 Gy) and injected with 4×10^6 bone marrow cells isolated from male GFP mice or MIP-GFP mice. We induced diabetes by STZ injection 4 weeks after BMT; analysis was performed 8 weeks later.

Confocal Laser Scanning Microscopy with Spectral Imaging Analysis. Mice were perfused with sterile saline via the left ventricle to wash out the blood. We took out the liver and pancreas and froze them in liquid nitrogen. Five-micron-thick frozen sections were cut in a cryostat and embedded on MAS-coated glass slides. Embedded sections were fixed with 1% paraformaldehyde (PFA) in 0.1M PBS for 15 min at 4°C, washed several times with PBS. Some sections were immediately observed under confocal laser scanning microscopy (C1si; Nikon Instech) to detect GFP fluorescence, other sections were processed for immunofluorescence-overlap staining.

For immunofluorescence-overlap staining, fixed sections were incubated with the mixture of antibodies against proinsulin (guinea pig polyclonal; Progen Biotechnik, Heidelberg, Germany) and TNF-α (goat polyclonal; Santa Cruz Biotechnology, Santa Cruz, CA), or incubated with antibody against β-gal (rabbit polyclonal; Biogenesis, Poole, U.K.) diluted 1:1,000 in PBS for 2 h at room temperature (RT). Sections were washed with PBS and further incubated with the mixture of FITC-labeled anti-guinea pig IgG (Chemicon, Temecula, CA) and Cy3-labeled anti-goat IgG (Chemicon) or incubated with Cy3-labeled anti-rabbit IgG (Chemicon) diluted 1:1,000 in PBS for 1.5 h at RT. In some sections, nuclei were stained with TO-PRO-3 iodide. Finally, sections were observed under confocal laser scanning microscopy (C1si or LSM 510; Nikon, Carl Zeiss). To further define the specificity of the immunolabeling, sections were stained with fluorescence-labeled second antibody without first antibody.

Spectrum imaging analysis combined with confocal laser scanning microscopy (C1si; Nikon) was applied on GFP-expressing cells or multicolor stained cells. Excitation wavelength was set at 488 nm for nonstained sections, whereas it was set at 488/543 nm for immunofluorescence overlap-stained sections. To clarify GFP-expressing or specific immunopositive cells from autofluorescence, an emission profile of the fluorescence was obtained from each structure seen under confocal laser microscopy.

Quantitative Morphometry of Proinsulin- or TNF-α-Positive Cells. Fluorescence-positive images detected under laser scanning microscopy were transmitted to the image-analyzing system MetaMorph (Ver. 4.6; Nippon Roper, Chiba, Japan). A mean value of area percentage of positive cells in the liver of each animal was determined by sampling from seven sections at $\times$20

objective; values represent the mean ± SD of data from three animals.

Analysis for Tissue mRNA Expression. Liver from STZ-diabetic and nondiabetic wild-type mice was homogenized in acid guanidinium-phenol-chloroform (TRIzol; Invitrogen, Carlsbad, CA); we then extracted and analyzed the total RNA by RT-PCR. We detected Ins1 transcript by RT-PCR using 35 cycles and TNF-α transcript by RT-PCR using 30 cycles. PCR products were confirmed by direct sequencing.

FISH for Y Chromosome Staining. Liver sample quick-frozen in liquid nitrogen was cut into 5-μm-thick sections and mounted on MAS-coated glass slides. Sections were fixed with 1% PFA in sterile saline for 15 min at 4°C, washed with deionized water, and incubated with 0.01% pepsin solution for 10 min at 37°C. Sections were washed with SSC, dehydrated with series of ethanol, and air dried. They were denaturated by 70% formamide solution for 15 sec at 65°C, dehydrated by series of ethanol, and air dried. The sections were covered with denatured hybridization probe (FITC-labeled mouse chromosome Y paint probe; ID Labs, London, ON, Canada) and incubated overnight at 37°C. We then incubated the sections further with 60% formamide solution for 15 min at 37°C and washed them with 0.05% Tween-20 solution. The sections were then incubated with either antibody against β-gal (rabbit polyclonal) or albumin (rabbit polyclonal; Biogenesis) diluted at 1:1,000 for 2 h at RT, further incubated with Cy3-labeled anti-rabbit IgG (Chemicon) diluted at 1:1,000 for 1.5 h at RT, and finally stained with DAPI for nuclear staining. We obtained the fluoresce image under a fluorescence microscope (BZ-8000; Keyence, Osaka, Japan).

Laser Capture Microdissection (LCM) and Quantitative Real-Time PCR. Snap-frozen liver and pancreas samples were cut into 5-μm sections. We mounted the sections on precleaned noncoated glass slides, fixed them with 0.4% PFA in sterile saline for 5 min at 4°C, and dehydrated them with series of ethanol and xylene and then air dried and used them for LCM (Arcturus, Pixcell IIe; Arcturus BioScience, Mountain View, CA). The image was observed under a fluorescence microscope attached to the LCM system at an excitation wavelength of 488 nm. GFP-positive cells, autofluorescent cells, and GFP-negative cells were captured from the livers of STZ-diabetic MIP-GFP mice, and autofluorescent and GFP-negative cells were captured from the livers of nondiabetic MIP-GFP mice. GFP-positive cells were captured from the pancreatic islets of nondiabetic MIP-GFP mice as controls. We used the following parameters on LCM system: power, 70 mW; pulse duration, 0.8 msec; spot size, 7.5 μm. Fifty to 70 captured cells on a single CapSure Macro LCM cap (Arcturus) were processed for mRNA extraction by using PicoPure RNA isolation kit (Arcturus).

After mRNA extraction, we synthesized cDNA using SuperScript II reverse transcriptase (Invitrogen) and performed quantitative real-time PCR with the LightCycler Fast Start DNA Master SYBR green I kit (Roche Diagnostics, Indianapolis, IN). The PCR mixture contained 20 ng of cDNA and the primers. Emitted fluorescence for each reaction was measured three times during the annealing/extraction phase, and amplification plots were analyzed by using LIGHTCYCLER software, Ver. 3.4 (Roche Diagnostics). The relative value in each sample was calculated by a standard curve obtained from control samples (GFP and Ins1 from pancreatic β cells, TNF-α from LPS (100 mg/kg)-treated liver), and data were standardized as quotient divided by the value simultaneously obtained for GAPDH in the same experiment. We showed their values by the percentage of β cells for GFP and Ins1, or by percentage LPS-treated liver for TNF-α. We also showed representative gel analysis of GFP, Ins1, and TNF-α products RT-PCR (37 cycles).

Insulin Treatment. Diabetes was induced by i.p. STZ (150 mg/kg). Two days after STZ, we inserted s.c. an insulin pellet in half of the animals and measured blood glucose levels once a week. Additional pellets were implanted when the blood glucose level went up to >200 mg/dl. Both STZ-treated and STZ+insulin-treated animals were killed for immunofluorescence-overlap staining and quantitative morphometry for Proins- and TNF-α-positive cells in the liver at 2 months after STZ.

Statistical Analysis. Two-way ANOVA, followed by a Bonferroni/Dunn test, was used to assess differences among groups. $P < 0.05$ was taken as statistically significant.

We thank Takefumi Yamamoto, Yasuhiro Mori, Miwako Katagi, Naoki Hayashi, Hiroyuki Sugihara, Mikiko Yoshikawa, and Masaki Masuda for technical support and Ryuichi Kikkawa for advice. This work was supported by Grant-in-Aid for Exploratory Research 17659383 (to M.F.) and Grant-in-Aid for Scientific Research 18390100 (to H. Kojima) from the Ministry of Education, Culture, Sports, Science, and Technology, Japan; President's Discretionary Fund from Shiga University of Medical Science Grant 1515143 (to H. Kojima); National Institutes of Health Grants DK68037 and HL51586; and from James and Lydia Chao and the TTWFC Global Foundation (to L.C.).

1. Wang X, Willenbring H, Akkari Y, Torimaru Y, Foster M, al-Dhalimy M, Lagasse E, Finegold M, Olson S, Grompe M (2003) *Nature* 422:897–900.
2. Vassllopoulos G, Wang P-R, Russell DW (2003) *Nature* 422:901–904.
3. Alvarez-Dolado M, Pardal R, Garcia-Verdugo JM, Fike JR, Lee HO, Pfeffer K, Lois C, Morrison SJ, Alvarez-Buylla A (2003) *Nature* 425:968–973.
4. Camargo FD, Finegold M, Goodell MA (2004) *J Clin Invest* 113:1266–1270.
5. Thorgeirsson SS, Grisham JW (2006) *Hepatology* 43:2–8.
6. Kojima H, Fujimiya M, Matsumura K, Nakahara T, Hara M, Chan L (2004) *Proc Natl Acad Sci USA* 101:2458–2463.
7. Oh S-H Muzzonigro TM, Bae S-H, LaPlante JM, Hatch HM, Petersen BE (2004) *Lab Invest* 84:607–617.
8. American College of Physicians (ACP); PIER (Physicians' Information and Education Resource); MKSAP (Medical Knowledge and Self Assessment Program) (2007) *Ann Int Med*, ed Laine C, 146:ITC1–15.
9. Hara M, Wang X, Kawamura T, Bindokas VP, Dizon RF, Alcoser SY, Magnuson MA, Bell G (2003) *Am J Physiol* 284:E177–E183.
10. Terashima T, Kojima H, Fujimiya M, Matsumura K, Oi J, Hara M, Kashiwagi A, Kimura H, Yasuda H, Chan L (2005) *Proc Natl Acad Sci USA* 102:12525–12530.
11. Baigorri F, Barkin JS (2003) in *Ellenberg & Rifkin's Diabetes Mellitus*, eds Porte D, Jr, Sherwin RS, Baron S (McGraw–Hill, New York), pp 879–894.
12. Ravikumar B, Carey PE, Snaar JE, Deelchand DK, Cook DB, Neely RD, English PT, Firbank MJ, Morris PG, Taylor R (2005) *Am J Physiol* 288:E789–E797.
13. Falchuk KR, Fiske SC, Haggitt RC, Federman M, Trey C (1980) *Gastroenterology* 78:535–541.
14. Adami H, Chow WH, Nyren O, Berne C, Linet MS, Ekbom A, Wolk A, McLaughlin JK, Fraumeni JF, Jr (1996) *J Natl Cancer Inst* 88:1472–1477.
15. Wideroff L, Gridley G, Mellemkjaer L, Chow WH, Linet M, Keehn S, Borch-Johnsen K, Olsen JH (1997) *J Natl Cancer Inst* 89:1360–1365.
16. Lagiou P, Kuper H, Stuver SO, Tzonou A, Trichopoulos D, Adami HO (2000) *J Natl Cancer Inst* 92:1096–1099.
17. Duelli D, Lazebnik Y (2003) *Cancer Cell* 3:445–448.
18. Bjerkvig R, Tysnes BB, Aboody KS, Najbauer J, Terzis AJA (2005) *Nat Rev Cancer* 5:996.
19. Pawelek JM (2005) *Lancet Oncol* 6:988–993.
20. Weimann JM, Jahansson CB, Trejo A, Blau HM (2003) *Nat Cell Biol* 5:959–966.
21. Weimann JM, Charlton CA, Brazelton TR, Hackman RC, Blau HM (2003) *Proc Natl Acad Sci USA* 100:2088–2093.
22. Friedl P (2005) *Lancet Oncol* 6:916–918.
23. Hernandez LD, Hoffman LR, Wolfsberg TG, White JM (1996) *Annu Rev Cell Dev Biol* 12:627–661.
24. Chen EH, Olson EN (2005) *Science* 308:369–373.
25. Ogle BM, Cascalho M, Platt JL (2005) *Nat Rev Mol Cell Biol* 6:567–575.
26. Chan L, Terashima T, Fujimiya M, Kojima H (2006) *Transact Am Clin Climatol Assoc* 117:341–352.
27. Kojima H, Fujimiya M, Terashima T, Kimura H, Chan L (2006) *Endocr J* 53:715–722.